THE JOURNAL OF COMPARATIVE NEUROLOGY 447:286–299 (2002)

Nigral and Pallidal Inputs to Functionally Segregated Thalamostriatal Neurons in the Centromedian/ Parafascicular Intralaminar Nuclear Complex in Monkey

MAMADOU SIDIBÉ, JEAN-FRANÇOIS PARÉ, AND YOLAND SMITH*
Yerkes Regional Primate Research Center and Department of Neurology, Emory University, Atlanta, Georgia 30322

ABSTRACT

In primates, thalamostriatal projections from the centromedian (CM) and parafascicular (Pf) nuclei are strong and organized according to a strict pattern of functional connectivity with various regions of the striatal complex. In turn, the CM/Pf complex receives a substantial innervation from the internal globus pallidus (GPi). In this study, we demonstrate that the substantia nigra pars reticulata (SNr) also provides a massive input to Pf in monkeys. These pallidothalamic and nigrothalamic projections provide routes whereby information can flow in functional loops between the basal ganglia and the intralaminar nuclear group. To understand better the anatomical organization and the degree of functional specificity of these loops, we combined retrograde and anterograde labeling methods from functionally defined regions of the striatum and GPi/SNr to determine the relationships between thalamostriatal neurons and basal ganglia afferents. Together with previous studies, our data suggest the existence of tightly connected functional circuits between the basal ganglia and the CM/Pf in primates: 1) A "sensorimotor" circuit links together the medial two-thirds of CM, the postcommissural putamen, and the ventrolateral part of the caudal GPi; 2) a "limbic" circuit involves the rostral one-third of Pf, the ventral striatum, and the rostromedial pole of GPi; and 3) an "associative"circuit exists between the caudal two-thirds of Pf, the caudate nucleus, and the SNr. An additional "associative" circuit that involves the caudate-receiving territory of GPi (dorsal one-third), the dorsolateral Pf (Pfdl), and the precommissural putamen was also disclosed. In conclusion, findings of this study provide additional evidence for the high degree of functional specificity of the thalamostriatal system through which CM/Pf may provide attention-specific sensory information important for conditional responses to the primate striatum. J. Comp. Neurol. 447:286–299, 2002.

Indexing terms: thalamostriatal projection; pallidothalamic projection; nigrothalamic projection; globus pallidus; substantia nigra

The intralaminar thalamic nuclei are part of the ascending reticular activating system, being particularly involved in cortical recruiting responses. On the basis of their relatively diffuse thalamocortical projections, the intralaminar nuclei are considered as nonspecific cell groups that activate broad cortical areas (Jones, 1985). However, this concept of nonspecificity is misleading when one examines the relationships between the intralaminar nuclei and the striatum, the other major target of this thalamic nuclear group (Groenewegen and Berendse, 1994). Various tract-tracing studies in rats, cats, and monkeys have, indeed, demonstrated that the thalamostriatal projections from the intralaminar nuclei are very specific in their pattern of distribution and synaptic connectivity (Sadikot et al., 1992a, b; Groenewegen and Berendse, 1994; Smith

Grant sponsor: NIH; Grant number: R01 NS37948-01; Grant number: RR00165.

*Correspondence to: Yoland Smith, Yerkes Primate Center, Emory University, 954 Gatewood Rd. NE, Atlanta, GA 30322.
E-mail: yolands@rmy.emory.edu

Received 23 October 2001; Revised 10 January 2002; Accepted 5 February 2002

DOI 10.1002/cne.10247

Published online the week of April 22, 2002 in Wiley InterScience (www.interscience.wiley.com).

et al., 1994; Gimenez-Amaya et al., 1995; Sidibé and Smith, 1996; Groenewegen et al., 1999; Mengual et al., 1999). In primates, the caudal intralaminar nuclear group, which comprises the centromedian (CM) and parafascicular (Pf) nuclei, is the main source of thalamic inputs to the striatum (Powel and Cowan, 1956; Parent and DeBellefeuille, 1983; Smith and Parent, 1986). Both nuclei project massively and topographically to the whole striatum according to the strict functional compartimentation of striatal territories (Nakano et al., 1990; Fenelon et al., 1991; Sadikot et al., 1992a,b). For instance, the CM innervates almost exclusively the postcommissural putamen, known as the sensorimotor striatal region, whereas the Pf is mainly connected with the precommissural putamen, caudate nucleus, and nucleus accumbens, considered as the associative and limbic striatal regions (Sadikot et al., 1992b; Gimenez-Amaya et al., 1995). In turn, basal ganglia output reaches intralaminar thalamic nuclei via projections through the internal pallidal segment (GPi). Although the GPi projection to the intralaminar nuclei have long been thought to target selectively the CM, we recently showed that both CM and Pf receive substantial inputs from the GPi in monkeys (Sidibé et al., 1997). The pallidointralaminar projection follows a pattern of functional organization in CM/Pf; i.e., the sensorimotor territory of GPi terminates preferentially in CM, whereas the associative and limbic GPi innervate preferentially Pf (Sidibé et al., 1997). Another major output structure of the basal ganglia is the substantia nigra pars reticulata (SNr). In rats, an SNr projection to Pf has been shown, but the extent and exact termination site of this projection in monkeys remain to be established (Beckstead et al., 1979; Gerfen et al., 1982; Ilinsky et al., 1985; Mengual et al., 1999).

To understand better the functional interactions between basal ganglia and thalamostriatal neurons in CM/Pf, our goal for the present study was to elucidate the synaptic and topographic relationships between functionally segregated basal ganglia output neurons from GPi/SNr and thalamostriatal neurons in monkeys. Results of this study have been presented previously in preliminary form (Smith and Sidibé, 1999; Smith et al., 2000; Sidibé et al., in press).

Abbreviations

AC	anterior commissure
CD	caudate nucleus
CM	centromedian nucleus
CP	cerebral peduncle
den	dendritic shaft
denv	vesicle-filled dendrite
FR	fasciculus retroflexus
FRTM	formatio reticularis tegmenti mesencephali
GPe	globus pallidus, external segment
GPi	globus pallidus, internal segment
IC	internal capsule
IP	interpeduncular nucleus
III	third ventricle
MD	mediodorsal nucleus
MG	medial geniculate body (nucleus)
NCP	nucleus commissurae posteriosis
PF, Pf	parafascicular nucleus
PFdl	parafascicular nucleus, dorsolateral part
PU	putamen
RN	red nucleus
SNc	substantia nigra, pars compacta
SNr	substantia nigra, pars reticulata
SPF	subparafascicular nucleus
STN	subthalamic nucleus
VPM	ventral posterior medial nucleus
VPL	ventral posterior lateral nucleus
VTA	ventral tegmental area
VS	ventral striatum
ZI	zona incerta

TABLE 1. Summary of Tracer Injections in the GPi, SNr and Straitum

	Tracer Injections		
Animals	GPi	SNr	Striatum
M39L*	BDA (Sensorimotor)	XXX	WGA/HRP-Post-com.Put
M39R*	BDA (Associative)	XXX	WGA/HRP-CD
M50L	BDA (Associative)	XXX	CTB-Post-com.Put
M50R	BDA (Associative)	XXX	CTB-D
M56L*	BDA (Associative)	XXX	WGA/HRP-Pre-com.Put.
M56R	BDA (Associative)	XXX	WGA/HRP-Pre-com.Put
M59L	XXX	BDA	WGA-HRP-CD
M59R	XXX	BDA	WGA/HRP-CD
M65L*	XXX	BDA	CTB-CD
M65R	XXX	BDA	CTB-CD

*Cases illustrated in Figure 6

MATERIALS AND METHODS

Animals, tracer injections, and perfuse fixation

In total five adult male squirrel monkeys were used in this study (Table 1). The anesthesia, surgical procedures, postoperative care, and perfusion of the animals were performed in accordance with the NIH Guide for the Care and Use of Laboratory Animals (1996) and the Emory University Animal Care and Use Committee. Surgical procedures were carried out with the animals under isoflurane anesthesia; animals were deeply anesthetized with an overdose of pentobarbital (100 mg/kg. iv) for perfusion.

In three monkeys (six hemispheres), bilateral iontophoretic injections of BDA (5% in distilled water; Molecular Probes, Eugene, OR) were placed in GPi while pressure injections of WGA-HRP (5% in 0.9% saline; Sigma, St. Louis, MO) or cholera toxin B subunit (Ctb, 5% in distilled water; List Biological Labs, Campbell, CA) were delivered in the striatum (Table 1). In brief, BDA injections were made through glass micropipettes with a tip diameter ranging from 20 to 50 μm using a 6 μA positive current delivered according to a 7 second on/7 second off cycle for 20 minutes. Six to eight days later, animals received pressure injections of WGA-HRP in the striatum through a 1 μl Hamilton microsyringe. In total, 0.2 μl of WGA-HRP and 0.3–0.6 μl of CTb were delivered at two sites along a single track through the striatum. Forty-eight hours after WGA-HRP injections or 5–6 days following injections of CTb, animals were deeply anesthetized and perfused transcardially with 300 ml of oxygenated Ringer's solution, followed by 800 ml of fixative containing 4% paraformaldehyde and 0.1% glutaraldehyde in phosphate buffer (PB; 0.1 M, pH 7.4). Free aldehydes were then removed by perfusion of 1 liter of PB (0.1 M, pH 7.4). All solutions were at 4°C. The brains were cut in 10-mm-thick blocks, taken out from the skull, and cut in 60-μm-thick sections with a vibrating microtome. Sections were then processed to reveal WGA-HRP or CTb and BDA according to protocols described below.

Two monkeys (four hemispheres) received bilateral BDA injections in the substantia nigra while CTb was injected in the caudate nucleus (Table 1). The perfusion

procedures were the same as described above. After the brains had been cut, sections were processed to reveal BDA and CTb according to the protocol described below. For each animal, a series of sections at the level of the injection sites and the CM/Pf was mounted on slides and Nissl stained with thionin.

BDA/WGA-HRP protocol

Sections prepared for light microscopy were first put in a 1% sodium borohydride solution for 20 minutes, washed thoroughly in phosphate-buffered saline (PBS; 0.01 M, pH 7.4), and then processed to reveal WGA-HRP according to the protocol of Olucha et al. (1985). Sections were first washed in cold PB (0.1 M, pH 6.2) before being put in the same buffer containing 0.25% ammonium molybdate (VI) tetrahydrate (Aldrich Chemical Co., Milwaukee, WI) and 0.5% of 3,3′,5,5′-tetramethylbenzidine (TMB). After a prereaction of 5 minutes, 0.003% hydrogen peroxide was added to the solution every 5 minutes throughout the incubation time of 30–35 minutes. The sections were then washed many times in PB (0.1 M, pH 6.2), and the TMB reaction product was stabilized for 6–8 minutes in a mixture of diaminobenzidine (DAB) and H_2O_2 as described by Rye et al. (1984). After the WGA-HRP had been revealed, sections were incubated overnight at room temperature in avidin biotin-peroxidase complex (ABC 1:100; Vector Laboratories, Burlingame, CA) containing 0.3% Triton X-100 and 1% bovine serum albumin (BSA) to localize BDA. This was followed by a 10 minute incubation in a mixture of DAB, 0.01 M imidazole, and H_2O_2. These sections were then put on gelatin-coated slides and air dried, and a coverslip was applied with Permount.

After incubation in sodium borohydride, sections prepared for electron microscopy were put in a cryoprotectant solution (25% sucrose, 10% glycerol in PB 0.05 M, pH 7.4) for 20 minutes and frozen at −80°C. They were then thawed in a graded series of diluted cryoprotectant solution, washed in PBS, and processed to reveal WGA-HRP and BDA according to the protocol described above, except that Triton X-100 was not added to the ABC solution. These sections were then prepared for electron microscopy.

BDA/CTb protocol

Sections prepared for light microscopy were first processed to reveal BDA with DAB and then preincubated in a mixture of 1% normal rabbit serum and 0.3% Triton X-100 for 30 minutes before being incubated with a goat anti-CTb antiserum (1:20,000; List Biological Laboratories) for 48 hours at 4°C. They were then incubated in biotinylated rabbit anti-goat IgGs (1:200; Vector Laboratories) for 90 minutes at room temperature, followed by an additional 90 minute incubation in ABC (1:100). After washes in PBS and Tris buffer (0.05 M, pH 7.6), the CTb was revealed with nickel-enhanced DAB by incubation in a mixture of DAB (0.025%), ammonium nickel sulfate (0.35%; Fisher Scientific, Fair Lawn, NJ), and hydrogen peroxide (0.0006%) for 10 minutes. The reaction was stopped by extensive washings in PBS. Sections were then mounted on slides and air dried, and a coverslip was applied with Permount.

Sections prepared for electron microscopy were processed according to the same protocol, except that Triton X-100 was omitted from the incubation solutions. After the reactions had been completed, sections were prepared for electron microscopy.

As controls, sections were processed to reveal BDA and incubated in a solution that contained nonimmune goat serum rather than goat anti-CTb antibodies. The rest of the protocol was the same as described above. In those sections, the CM/Pf was devoid of retrogradely labeled elements but still contained BDA-positive terminals.

Preparation of tissue for electron microscopy

The sections were washed in PB (0.1 M, pH 7.4) before being postfixed in osmium tetroxide (1% solution in PB) for 20 minutes. They were then dehydrated in a graded series of alcohol and propylene oxide. Uranyl acetate was added to the 70% ethanol (30 minutes) to improve the contrast in the electron microscope. The sections were then embedded in resin (Durcupan ACM; Fluka EM Sciences, Fort Washington, PA) on microscope slides and put in the oven for 48 hours at 60°C. After a detailed examination in the light microscope, regions of interest in CM/Pf were drawn, sometimes photographed, cut out from the slides, and glued on the top of resin blocks with cyanoacrylate glue. Serial ultrathin sections were cut on a Reichert-Jung Ultracut T2 ultramicrotome (Leica, Nussloch, Germany) and collected on Pioloform-coated single-slots copper grids. They were stained with lead citrate (Reynolds, 1963) and examined with a Zeiss EM-10C electron microscope (Thornwood, NY).

Analysis of material

The location and extent of injection sites as well as the distribution of retrograde and anterograde labeling in the thalamus and striatum were charted from coronal sections at 1.6× and 2.5× magnifications with a drawing tube connected to a Leitz light microscope. Thionin-stained sections were used to delineate the limits of CM/Pf.

The synaptic relationships between anterogradely labeled terminals and retrogradely labeled cells in CM/Pf were studied as follows. Blocks of tissue were selected from areas of overlap of retrograde and anterograde labeling in CM/Pf. Ultrathin sections from the surface of the blocks were put on grids and scanned in the electron microscope for BDA-labeled terminals. After a labeled terminal was found, it was photographed at low (16,000×) and high (31,500×) magnifications. The type of synapses established by these terminals was categorized as symmetric or asymmetric, and the ultrastructural features of the postsynaptic targets were determined. To make sure that the labeling was optimal to find synaptic interactions between anterogradely labeled terminals and retrogradely labeled cells, we considered only those BDA-labeled terminals that occurred in a field that also contained retrogradely labeled elements. Furthermore, in cases in which anterogradely labeled boutons were close or apposed to retrogradely labeled structures, they were examined through serial ultrathin sections to determine the existence of synaptic contacts.

RESULTS

Nomenclature of the CM/Pf nuclear complex

The nomenclature of CM/Pf subnuclei used in the present study was described in detail in our previous analysis of the pallidothalamic projection (Sidibé et al., 1997). In brief, the CM/Pf is subdivided into three major parts based on cytological and hodological features. The Pf

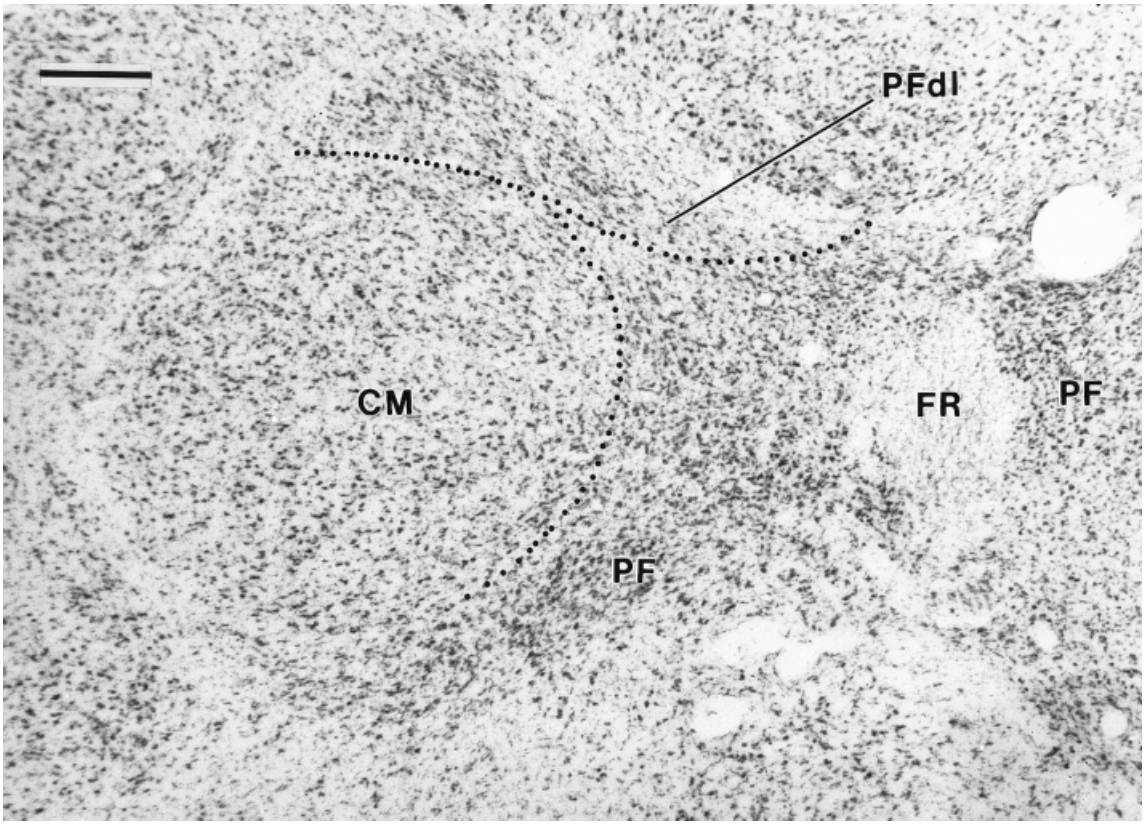

Fig. 1. Nissl-stained section of the CM/Pf nuclear complex shows the different nuclei subdivisions. Scale bar = 0.5 mm.

is identified as the medialmost region of the complex that contains densely packed, small, round perikarya. This nucleus can be easily differentiated from the CM, which is located more laterally and contains a lower density of cells that appear paler in Nissl-stained preparations (Fig. 1). In the middle and caudal one-thirds of the nuclear complex, a third subnucleus that we refer to as the *dorsolateral part of the Pf* (Pfdl) was identified. This region is characterized by densely packed fusiform perikarya oriented in the mediolateral plane (Sidibé et al., 1997). The distinction between this nucleus and the medialmost region of the Pf or the underlying CM is clear in Nissl-stained material (Fig. 1).

SNr inputs to CM/Pf

In the two animals that received BDA injections in the SNr, the location of injection sites and resulting pattern of anterograde labeling in the thalamus were relatively similar. In both cases, the core of the injections was centered on the middle part of the SNr, though diffusion was found in the overlying SNc (Figs. 2, 3A). A large compact bundle of ascending anterogradely labeled fibers arose from these injection sites. These axons travelled rostrodorsally through the fields of Forel and gave rise to rich plexi of labeled varicosities in the subparafascicular nucleus rostrally (Fig. 2A). At middle and caudal levels of the CM/Pf complex, the labeling was found mainly in Pf (Figs. 2B–D, 3C). With the exception of a few sparsely distributed varicose fibers, the CM and Pfdl were almost completely devoid of labeling following these injections (Figs. 2B,C,

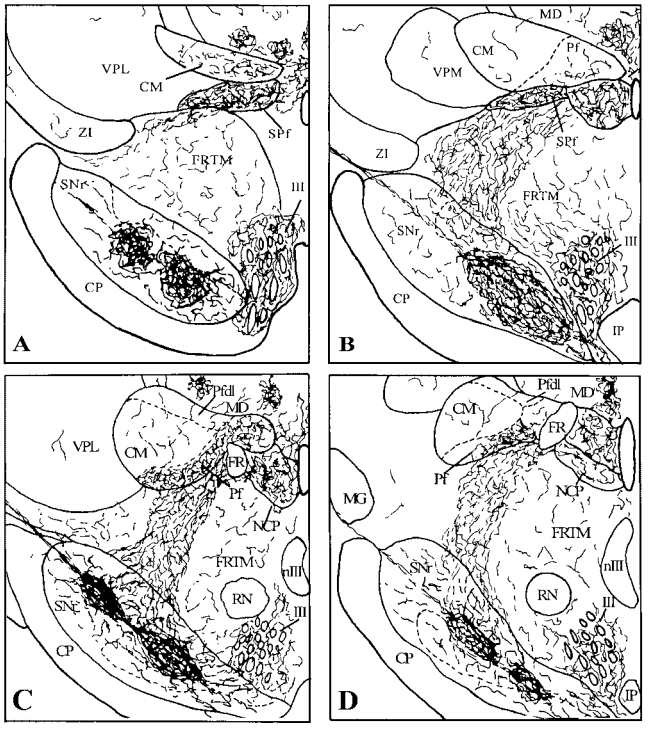

Fig. 2. Diagram showing the pattern of distribution of anterogradely labeled fibers and terminals through the rostrocaudal extent (**A–D**) of CM/Pf following BDA injections in the SNr.

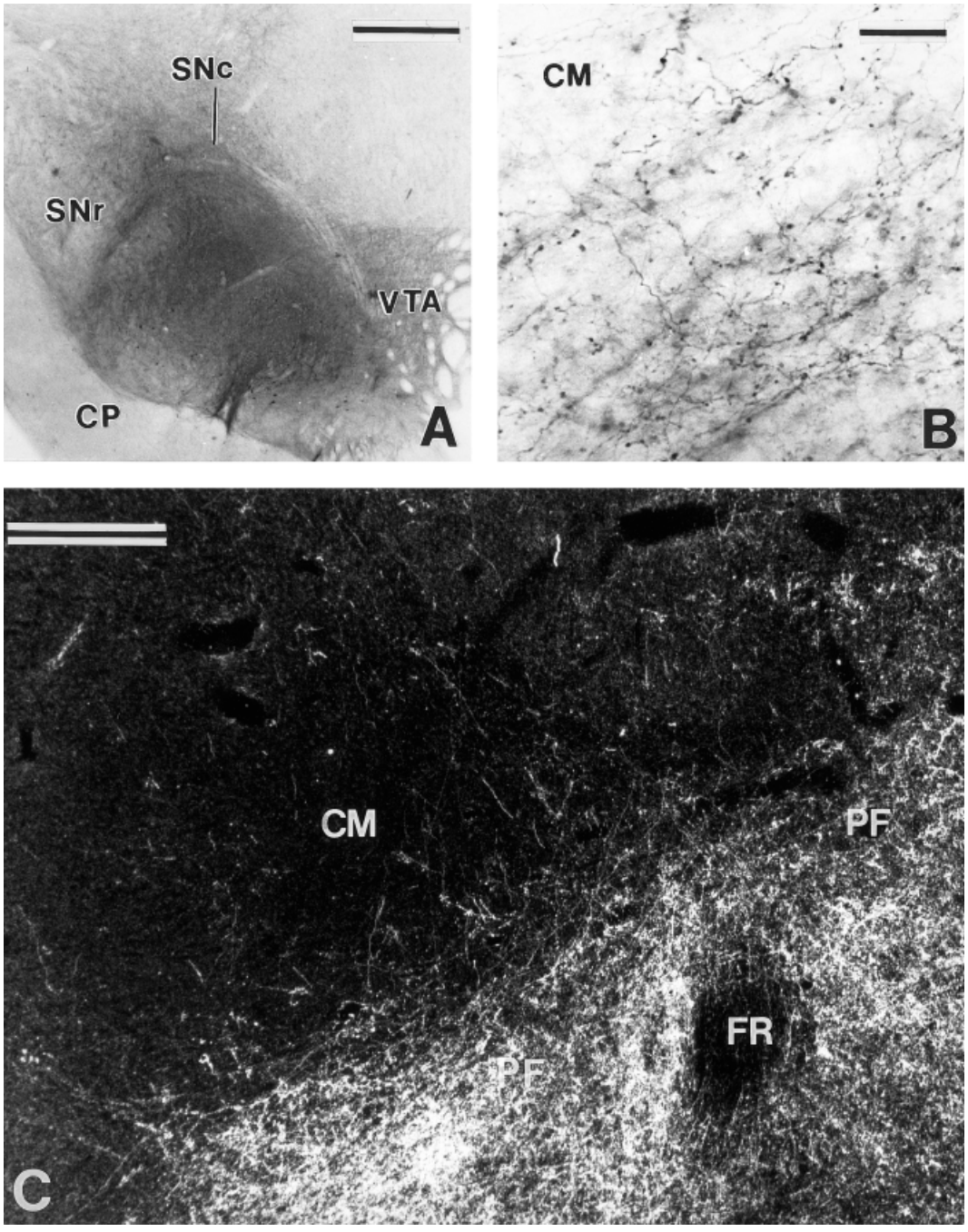

Fig. 3. Anterogradely labelled fibers in Pf after BDA injections in SNr. **A:** BDA injection site in SNr. **B:** High magnification of anterogradely labelled varicose fibers in Pf. **C:** Darkfield low-power view of anterograde labelling in Pf. Note the scarce labelling in CM and Pfdl. Scale bars = 0.5 mm in A,B, 1 mm in C.

3). Other thalamic nuclei, such as the mediodorsal and ventral anterior nuclei, which are known to receive inputs from the SNr, contained a moderate to large amount of labeling after these injections (Fig. 2).

Ultrastructural features of SNr inputs to Pf: a comparison with GPi inputs to CM and Pfdl

At the electron microscopic level, most SNr boutons were large (maximum diameter range from 1.2 to 2.2 μm), contained many mitochondria and pleomorphic electron-lucent vesicles as well as one or two dense-core vesicles, and formed predominantly symmetric synapses with dendrites of Pf neurons (Fig. 4). In addition, about 10% of anterogradely labeled terminals examined in Pf were smaller, contained round vesicles, and formed asymmetric axodendritic synapses (Fig. 4D). A particular feature that characterized both populations of labeled boutons was their preferential innervation of small dendrites. More than 70% of BDA-containing boutons examined estab-

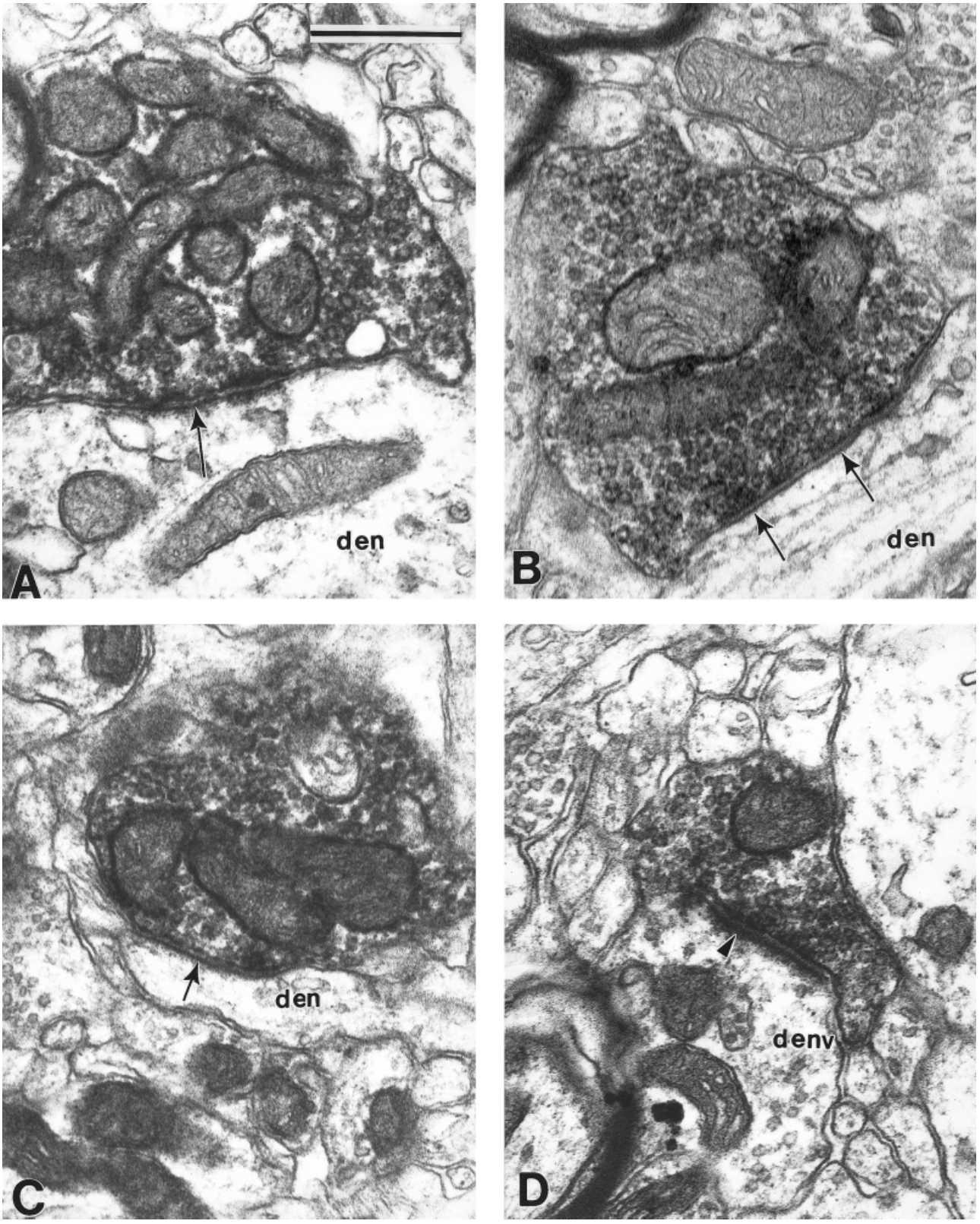

Fig. 4. Electron micrographs of anterogradely labeled SNr boutons forming symmetric synapses (**A–C**; arrows) with dendrites of various sizes in Pf. **D:** Another type of labeled bouton in Pf after BDA injection in SNr. This bouton forms an asymmetric synapse (arrowhead) with a vesicle-filled dendrite (denv) of an interneuron. Scale bar = 0.5 μm.

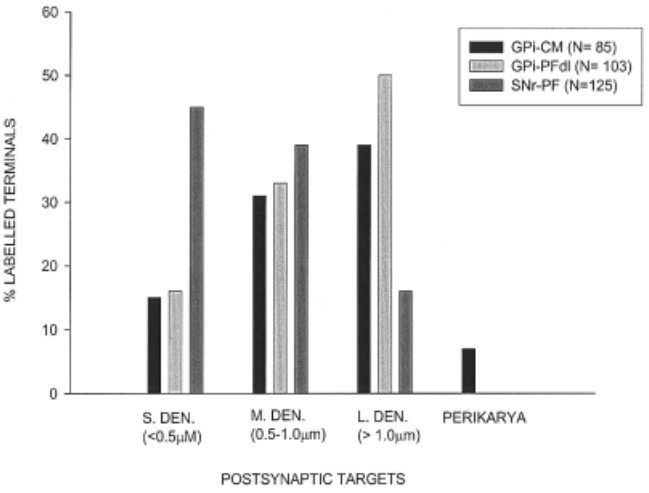

Fig. 5. Histogram comparing the relative distribution of postsynaptic targets of SNr boutons in Pf with that of GPi boutons in CM and Pfdl. Data for GPi terminals in CM are taken from Sidibé et al. (1997). Only boutons that form symmetric synapses are included in this histogram. The total number of boutons examined in each subnucleus is indicated in parentheses. Table 2 shows the amount of material that has been analyzed at the electron microscopic level in this study. Note that SNr boutons form synapses preferentially with small dendrites, whereas GPi terminals contact more proximal dendrites and perikarya.

lished symmetric synapses with dendrites less than 1.0 μm in diameter (Figs. 4, 5). Only 2 of the 125 SNr terminals examined contacted vesicle-filled dendrites, which suggests that output neurons are the main targets of SNr projections to Pf. Figure 5 shows a histogram that compares the distribution of postsynaptic targets of SNr boutons in Pf with that of GPi terminals in CM and Pfdl. In contrast to SNr terminals, the majority of GPi boutons form symmetric synapses with large dendrites of CM and Pfdl neurons (Fig. 5), which indicates that the two basal ganglia output nuclei preferentially target different parts of the dendritic tree of CM/Pf neurons.

Basal ganglia inputs to thalamostriatal neurons

Light microscopic observations. After combined injections of retrograde tracers in the striatum with BDA injections in GPi or SNr, retrogradely labeled cells and anterogradely labeled terminals were found in CM/Pf. At the light microscopic level, the two sets of labeled elements were distinguishable by the color and texture of the reaction product associated with them; whereas the BDA-containing boutons displayed an amorphous brown deposit, the WGA-HRP and CTb labeling in CM/Pf neuronal perikarya was black and displayed a more granular appearance (Fig. 7). Overall, the pattern of distribution of retrogradely labeled cells and GPi terminals in CM/Pf was consistent with that reported in previous studies (Parent and DeBellefeuille, 1983; Smith and Parent, 1986, Sidibé et al., 1997). To characterize the functional relationships between thalamostriatal neurons and basal ganglia outputs, we mapped the distribution of retrogradely labeled cells and anterogradely labeled fibers throughout the rostrocaudal extent of CM/Pf (Fig. 6).

In one hemisphere (M39L), BDA was placed in the ventrolateral two-thirds of GPi while WGA-HRP was delivered in the postcommissural putamen (Fig. 6A–C). After such injections, clusters of BDA-containing cells were found throughout the postcommissural putamen in partial register with the WGA-HRP injection site. At the level of CM/Pf, WGA-HRP-labeled cells and BDA-containing varicosities tightly overlapped in the caudomedial two-thirds of CM, whereas the lateral edge of CM as well as Pf and Pfdl contained only a few, sparsely distributed BDA-positive fibers (Fig. 6A–C).

In two hemispheres (M39R and M50R), BDA was injected in the dorsal one-third of the rostral GPi while WGA-HRP or CTb was delivered in the head and body of the caudate nucleus. After such injections, BDA-containing cells were found in the caudate nucleus and the dorsomedial part of the rostral putamen close to the internal capsule (Fig. 6D–F). In CM/Pf, retrogradely labeled thalamostriatal neurons and anterogradely labeled GPi fibers were segregated; the BDA-labeled fibers were restricted to Pfdl, whereas most retrogradely labeled cells were confined to Pf (Figs. 6D–F, 7A,B). In two other hemispheres (M56L and M56R), BDA was injected in the dorsal half of the rostrolateral part of GPi while WGA-HRP was delivered in the precommissural putamen. These injections led to a tight overlap of labeled cells and terminals in the Pfdl (Figs. 6G–I, 7C,D). A few retrogradely labeled cells were also seen in the dorsomedial part of Pf, but the CM and the ventrolateral sector of Pf were completely devoid of labeling (Fig. 6G–I). Taken together, these findings, combined with those of our previous study (Sidibé et al., 1997), indicate that "associative" thalamostriatal neurons in Pf that project to the caudate nucleus receive few inputs from GPi.

Therefore, we tested in two more animals the possibility that the SNr was the main source of basal ganglia inputs to caudate-projecting thalamostriatal neurons in Pf. To do so, we injected four hemispheres (M59L, R and M65L, R) with WGA-HRP or CTb in the caudate nucleus combined with BDA injections in the SNr. After these injections, retrogradely labeled thalamocaudate neurons and anterogradely labeled nigrothalamic fibers tightly overlapped in the ventrolateral and medial pole of the caudal two-thirds of Pf (Figs. 6J–L, 7E,F). A few anterogradely labeled fibers, but no retrogradely labeled cells, were also seen in CM and Pfdl.

Electron microscopic observations. To ensure that the overlapping fields of retrogradely labeled cells and anterogradely labeled terminals in CM/Pf were sites of synaptic relationships between basal ganglia afferents and thalamostriatal neurons, we performed an electron microscopic analysis in cases M39L and M56L (Fig. 6A–C,G–I). The number of blocks and sections examined is shown in Table 2. With the electron microscope, BDA-containing terminals were easily distinguishable from the two retrograde markers based on the texture of the reaction product associated with them. The DAB deposit used to localize BDA had an amorphous texture, which filled quite homogeneously the anterogradely labeled terminals, whereas the TMB deposit used to reveal WGA-HRP displayed a crystalline texture (Fig. 8). On the other hand, the Ni-DAB used to localize CTb had the appearance of dark, electron-dense granules in retrogradely labeled elements. Most retrogradely labeled elements were large dendrites and perikarya. Dendrites smaller than 0.5 μm in diameter were generally devoid of WGA-HRP or CTb, suggesting that the retrograde markers were confined to the proximal part of labeled neurons. WGA-HRP- or CTb-

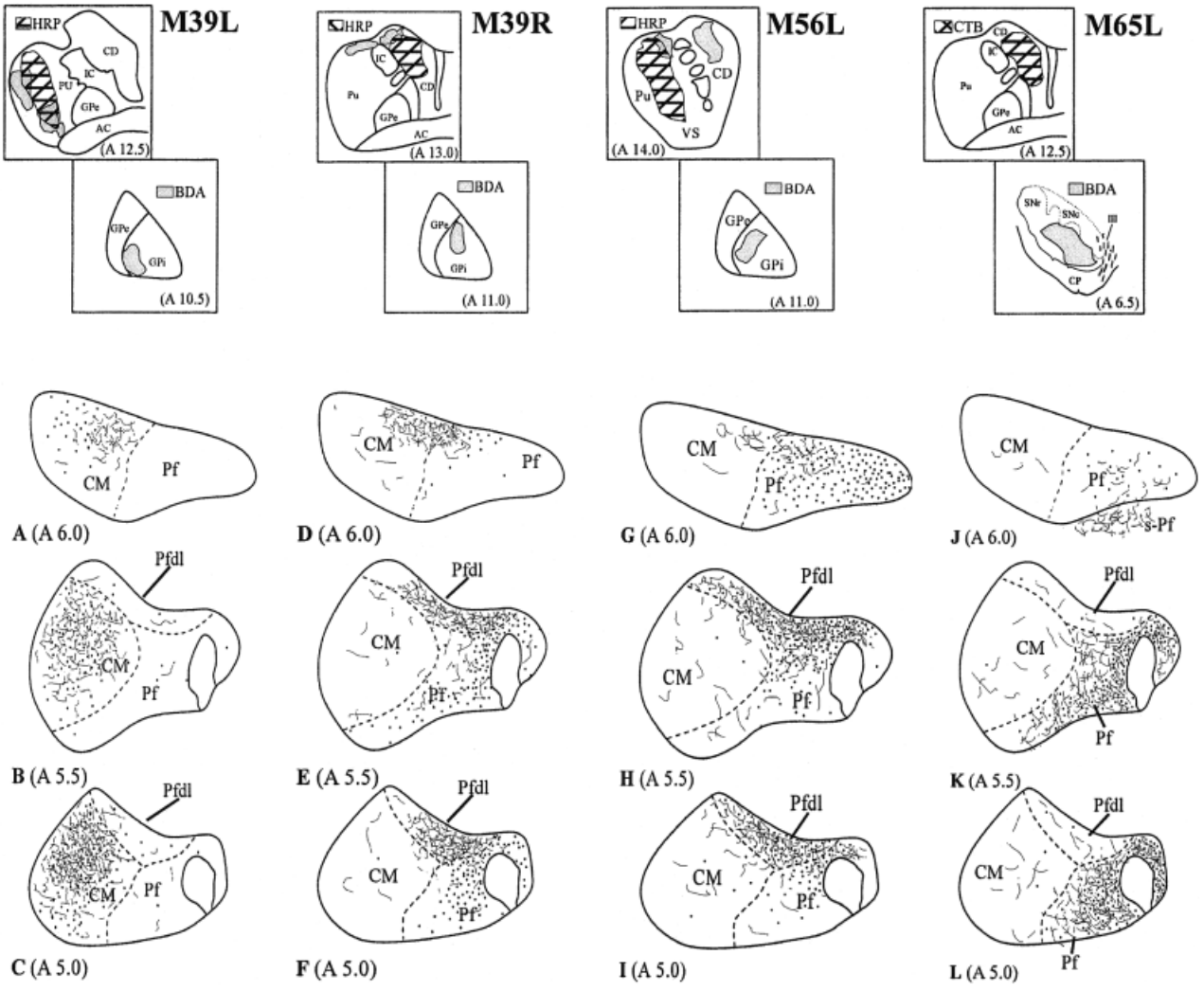

Fig. 6. Drawing to illustrate the pattern of distribution of anterogradely labeled fibers (sinuous lines) and retrogradely labeled cells (dots) in CM/Pf following BDA injections in GPi (**A–I**) or SNr (**J–L**) and WGA-HRP or CTb in the striatum. The anteroposterior stereotaxic coordinates corresponding to the level of injection sites in the striatum and GPi/SNr and the resulting labeling in CM/Pf are indicated in parentheses.

containing axons and axon terminals were not seen in any of the sections examined. Direct symmetric axodendritic synapses between retrogradely labeled dendrites and anterogradely labeled terminals were found in both regions (Fig. 8), indicating that functional synaptic relationships exist between basal ganglia outflow and thalamostriatal neurons in primates.

TABLE 2. Source and Amount of Tissue Examined at the Electron Microscopic Level

Animals	Areas examined	Number of blocks	Number of sections	Total number of BDA-containing boutons examined
M50R	Pfdl	3	44	55
M56R	Pfdl	5	66	48
M59R	Pf	3	40	70
M65L	Pf	6	73	55

DISCUSSION

The results of this study further emphasize the tight relationships between the basal ganglia and the caudal intralaminar thalamic nuclei, CM/Pf, in primates. Our findings demonstrate that both GPi and SNr have access to complementary regions of the CM/Pf complex. We propose, based on these data and those obtained in previous studies (Gimenez-Amaya et al., 1995; Sidibé et al., 1997), that the basal ganglia and CM/Pf largely interact via functionally segregated circuits in monkeys, including the following: 1) a "sensorimotor" circuit, which involves the ventrolateral GPi, the medial two-thirds of CM, and the postcommissural putamen; 2) a "limbic" circuit, which comprises the rostromedial pole of GPi or the ventral pallidum, the rostral two-thirds of the medial Pf, and the nucleus accumbens; and 3) two "associative" circuits; one between the SNr, the Pf, and the caudate nucleus and a second circuit between the dorsal one-third of GPi, the

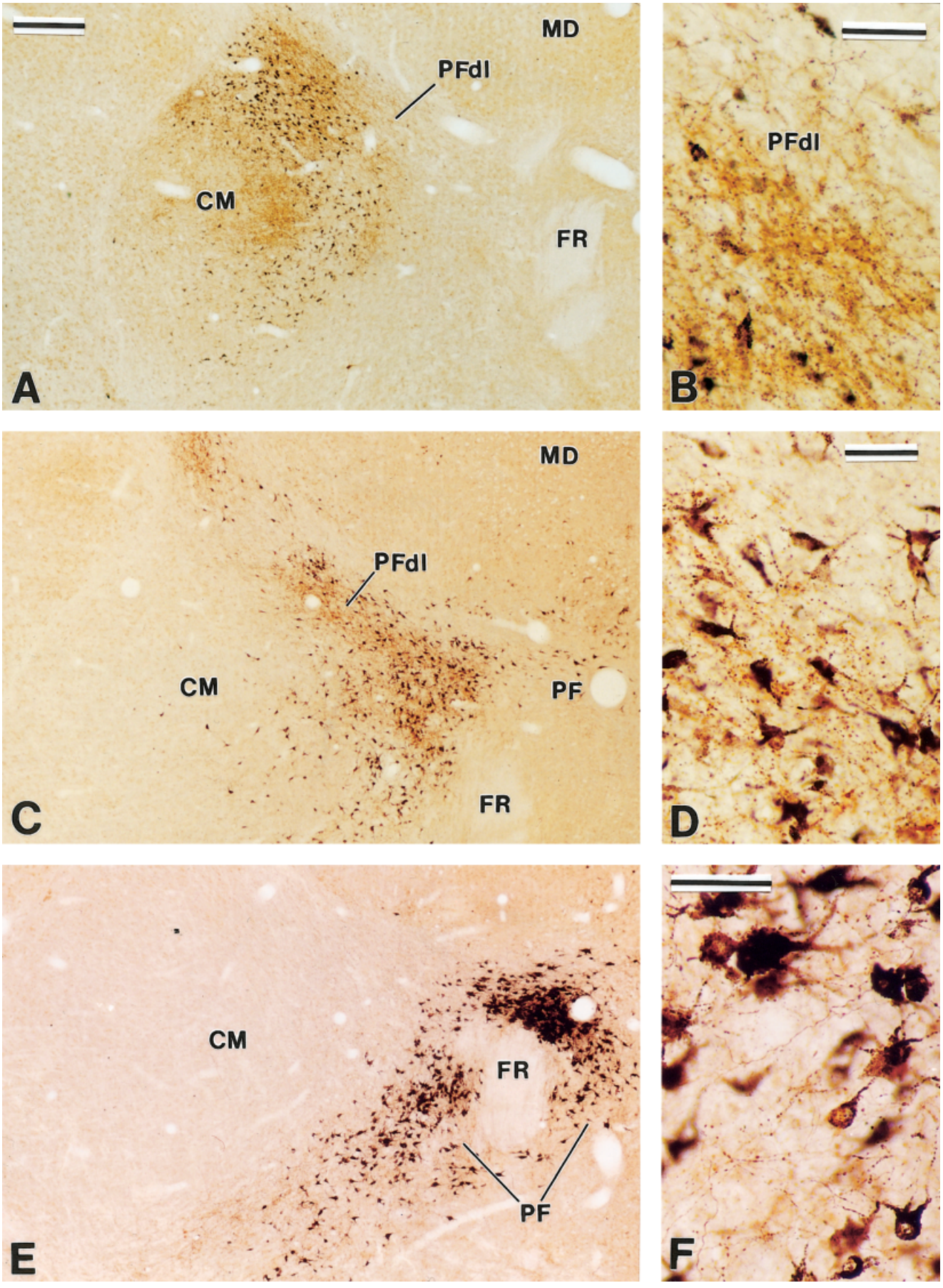

Fig. 7. Color light photomicrographs showing examples of retrograde and anterograde labeling in CM/Pf following BDA injections in GPi (**A–D**) or SNr (**E,F**) and WGA-HRP (A–D) or CTb (E,F) in different striatal regions. A and B show examples of HRP-labeled cells in register with anterogradely labeled fibers in CM in case M39L. C and D illustrate overlap of retrograde and anterograde labeling in Pfdl in case M56L. E and F depict retrogradely labeled cells in register with anterogradely labeled fibers in Pf in case M65L. Scale bar in A = 0.5 mm for A,C,E, in B = 100 μm, in D,F = 50 μm.

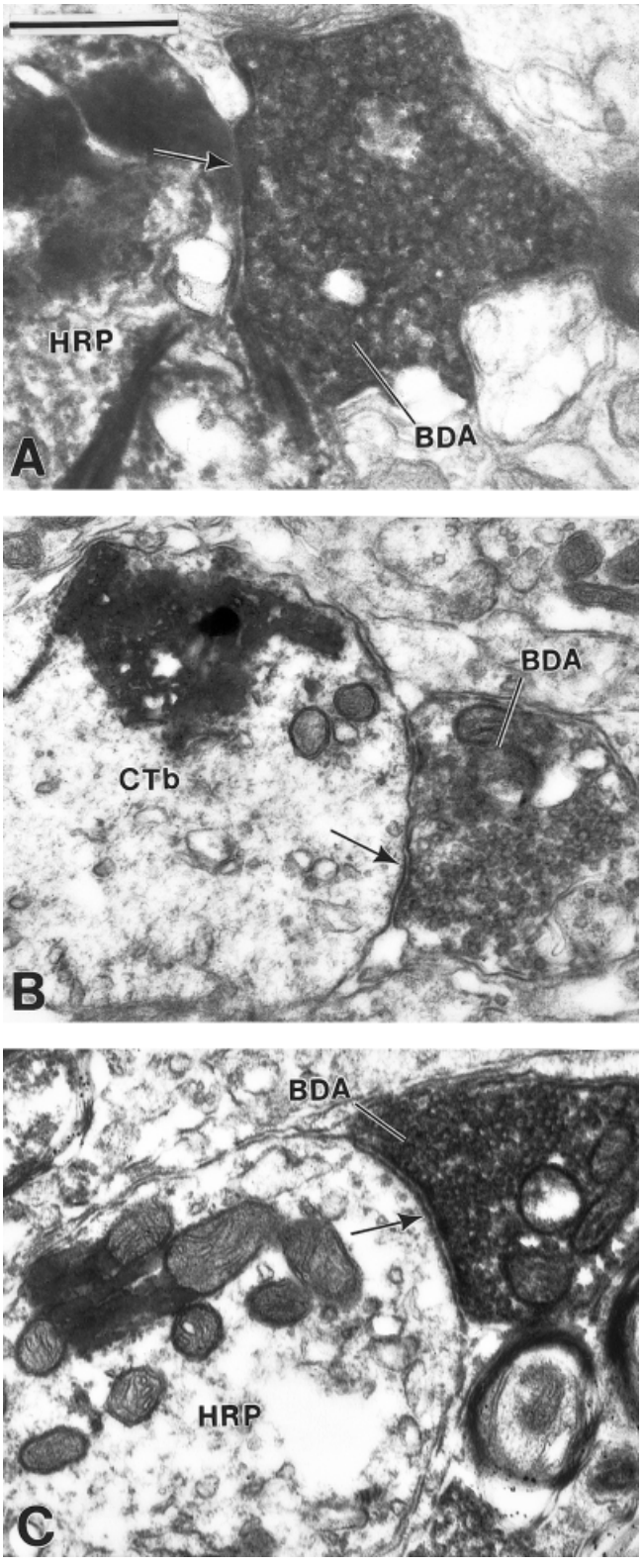

Fig. 8. Electron micrographs showing examples of symmetric synapses (arrows) between BDA-labeled boutons from GPi and WGA-HRP-labeled dendrites in CM (**A,B**) and Pfdl (**C**) in cases M39L (A,B) and M56L (C). Scale bar = 0.5 μm.

Pfdl, and the precommissural putamen (Fig. 9). These observations provide further evidence for the high degree of specificity of the so-called nonspecific caudal intralaminar thalamic nuclei (Groenewegen and Berendse, 1994). They also set the stage for additional studies of the role of CM/Pf in the functional circuitry of the primate basal ganglia under normal and pathological conditions.

Technical considerations

The interpretation of data obtained in this study relies on the sensitivity and specificity of the tract-tracing techniques and double-labeling methods used to differentiate GPi and SNr terminals from processes of thalamostriatal neurons at the light and electron microscopic levels in the CM/Pf complex. We believe that data presented in Figures 7 and 8 strongly support our conclusions on the existence of various basal ganglia functional loops through CM/Pf. One of the concerns about these findings could be the problem in differentiating retrogradely labeled cells from anterogradely labeled varicosities in CM/Pf at the light microscopic level (Fig. 7). Although the revelation of WGA-HRP resulted in a slightly darker peroxidase reaction product than the DAB staining in varicose fibers, this difference is relatively subtle and should be interpreted cautiously. In addition, the fact that WGA-HRP and BDA are transported in both retrograde and anterograde directions further indicates that great care should be taken in the interpretation of these data. However, despite these technical limitations, various observations made in this and previous studies strongly support the interpretation of our findings.

A first possibility to be examined is that some of the putative varicose axon terminals seen in CM/Pf result from the anterograde labeling of striatofugal axons by WGA-HRP rather than from BDA injections in GPi or SNr. This could, indeed, be the case if the striatum (where all WGA-HRP injections were made) had direct axonal projections to CM/Pf. However, such a connection has never been found in adult animals. Therefore, we believe that none or very few of the so-called BDA-containing fibers in CM/Pf arise from the striatum. In support of this is the fact that axon terminals labeled with crystals of WGA-HRP were not found in double-labeled sections at the electron microscopic level. All labeled boutons contained the amorphous DAB reaction product (Fig. 8). In addition, the pattern of distribution of the so-called BDA-containing fibers in CM/Pf in the double-labeled sections (WGA/HRP or CTB + BDA) was similar to that obtained in cases in which only BDA was injected in either GPi (Sidibé et al., 1997) or SNr (Figs. 2, 3). Together, these observations provide strong evidence to rule out the possibility that the anterogradely labeled fibers in CM/Pf arise from the striatum. Another potential source of the putative axon terminals seen in CM/Pf could be axon collaterals of retrogradely WGA-HRP-labeled thalamostriatal neurons. We believe this is likely not the case for the following reasons. If the terminals were collaterals of retrogradely labeled cells, they should contain crystals of WGA-HRP and form asymetric synapses (as is the case for glutamatergic thalamostriatal boutons; Sadikot et al., 1992b). As mentioned above, we did not find a single WGA-HRP-labeled bouton in the material that has been examined at the electron microscopic level. Furthermore, even if a small subset of labeled boutons, described in this study and our previous study (Sidibé et al., 1997), formed asymmetric synapses, these represented less than 10% of

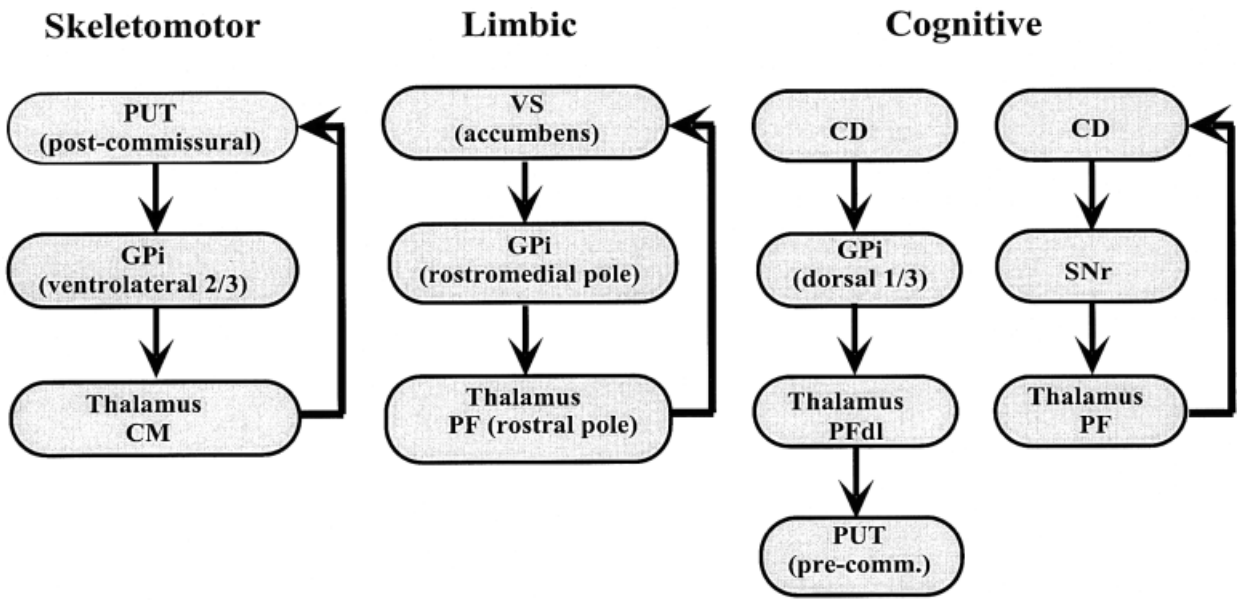

Fig. 9. Proposed functional circuits between the basal ganglia and the CM/Pf in monkeys based on data from this study and other studies (Gimenez-Amaya et al., 1995; Sidibé et al., 1997).

the total number of labeled terminals, and all of them contained the amorphous DAB reaction product, which indicates that they were labeled with BDA.

Both GPi and SNr have access to CM/Pf in monkeys

Although the GPi projection to CM/Pf has long been established in monkeys, such is not the case for the SNr. Nigral injections of tritiated amino acids resulted in scarce anterograde labeling, which was often attributed to fibers of passage, in the monkey Pf (Carpenter et al., 1976; Ilinsky et al., 1985; Francois et al., 1988). On the other hand, the existence of an SNr-Pf projection has been repeatedly demonstrated in other species by using anterograde and retrograde transport methods (Beckstead et al., 1979; Gerfen et al., 1982; Sakai and Smith, 1992; Sakai and Patton, 1993; De las Heras et al., 1998; Mengual et al., 1999; Tsumori et al., 2000). Our data clearly show that both GPi and SNr provide massive and complementary projections to the primate CM/Pf; the GPi projection is directed mainly to CM and Pfdl, whereas the SNr output innervates selectively the Pf (Sidibé et al; in press). Therefore, the two basal ganglia output structures innervate segregated territories of the CM/Pf complex in monkeys. These observations extend previous findings showing that nigral and pallidal afferents largely target different territories of the thalamic ventrobasal complex in monkeys (Ilinsky et al., 1985; Sakai et al., 1996, 2000). The functional implication of such segregation at the level of the ventrobasal complex is that nigral and pallidal outflows target different populations of thalamocortical neurons, the SNr being mostly linked with neurons that project to the premotor and anterior frontal cortices, whereas the GPi targets preferentially neurons that innervate the primary and supplementary motor areas (Ilinsky et al., 1985; Sakai et al., 2000). As shown in this study, the segregation of GPi and SNr inputs to CM/Pf implies that nigrofugal information is sent to the caudate nucleus, whereas GPi outflow is conveyed to the pre- and postcommissural putamen. However, we cannot rule out the possibility that basal ganglia projections also target CM and Pf neurons that project to the cerebral cortex or other subcortical structures. Whether these projections are collaterals of thalamostriatal axons or arise from separate neuronal populations remains to be established in primates. In rats and cats, double retrograde labeling studies revealed that cortical and striatal projections from CM/Pf arise largely from separate neuronal populations, whereas neurons in rostral intralaminar nuclei display a higher degree of axon collateralization (Royce, 1983; Macchi et al., 1984). On the other hand, recent single cell filling data suggest that both rostral and caudal intralaminar thalamic neurons project to both the striatum and the cerebral cortex in rats (Deschenes et al., 1996a,b). However, it is worth noting that rostral intralaminar neurons in the centrolateral nucleus project profusely to the cortex and send loosely organized axon collaterals in the striatum (Deschenes et al., 1996b), whereas caudal intralaminar neurons in Pf project massively to the striatum but also send thin axon collaterals to the motor cortex (Deschenes et al., 1996a). Studies are in progress to characterize the synaptic relationships between various groups of CM/Pf thalamofugal neurons and basal ganglia afferents in monkeys.

GPi and SNr inputs display a different pattern of synaptic innervation in CM/Pf

As shown in previous studies, GPi and SNr provide massive inhibitory inputs to segregated regions of the ventral anterior nucleus (VA)/ventral lateral (VL) nucleus in monkeys (Schell and Strick, 1984; Ilinsky et al., 1993). At the electron microscopic level, both inputs terminate preferentially on the cell body and primary dendrites of thalamocortical neurons (Ilinsky and Kultas-Ilinsky, 1990; Kultas-Ilinsky and Ilinsky, 1991). We have demonstrated, in line with these data, that GPi terminals form synapses preferentially with the proximal part of CM and

Pfdl neurons in squirrel monkeys (Sidibé et al., 1997). However, such is not the case for SNr boutons, which mostly contact small distal dendrites in the monkey Pf. Furthermore, none of the SNr boutons examined formed synapses with the soma of Pf neurons, another indication that these inputs are distally located. The functional impact of such a differential pattern of synaptic innervation of CM/Pf neurons by the two basal ganglia afferents is that the firing activity of CM and Pfdl neurons may be under the powerful control of proximal GPi inputs, whereas SNr afferents likely provide more subtle and specific modulatory influences of distal excitatory inputs to Pf neurons.

A rather surprising observation in the present study was the finding of a small subset of labeled boutons forming asymmetric synapses after BDA injections in the SNr. Such terminals have not been seen in the VAmc after tritiated amino acid injections in the macaque SNr (Kultas-Ilinsky and Ilinsky, 1990). The fact that asymmetric synapses are usually associated with excitatory synaptic inputs makes us believe that these boutons do not originate from GABAergic SNr neurons. The most likely explanation would be that BDA was taken up by ascending fibers from brainstem nuclei that pass through the substantia nigra (SN) to reach CM/Pf. These may include fibers from raphe, PPN, reticular formation, locus coeruleus, and other locations, which all provide thalamic inputs that form asymmetric synapses (Tseng and Royce, 1986; Hallanger et al., 1987; Paré et al., 1988; Liu and Jones, 1991; Royce et al., 1991; Balercia et al., 1996). It is worth noting that a few boutons forming asymmetric synapses were also found in CM after BDA injections in GPi (Sidibé et al., 1997). Even if the source of these boutons cannot be established, the fact that they represent a small proportion of the total pool of labeled terminals indicates that most BDA-containing boutons examined in these studies arose from basal ganglia output structures.

Functionally segregated circuits between the basal ganglia and the CM/Pf

The organization of the basal ganglia-thalamocortical loops is not fully understood and is still a matter of discussion. In 1986, Alexander and colleagues proposed the idea that the information flowing through the basal ganglia remains largely segregated in separate functional channels that include discrete, nonoverlapping parts of the striatum, globus pallidus, thalamus, and cerebral cortex. From the standpoint of information processing, this model suggests that the basal ganglia-thalamocortical circuits relay information around closed and completely isolated loops. Although this concept has been widely accepted, some investigators have provided evidence that challenges this model of organization and rather emphasizes the importance of convergent information that takes place in basal ganglia output structures (Percheron and Filion, 1991). Others have argued that integration of information between functionally segregated basal ganglia circuits may take place at different levels, including corticocortical, intrastriatal, and nigrostriatal connections (Joel and Weiner, 1994). The introduction of this model was based largely on anatomical and functional relationships between the striatopallidal complex, thalamocortical neurons in the ventrobasal nuclear group, and frontal cortical regions (Alexander et al., 1986). Over the past 10 years, it has become clear that the intralaminar nuclei provide highly specific and functionally segregated inputs to various striatal regions (Parent, 1990; Sadikot et al., 1992; Groenewegen and Berendse, 1994; Mengual et al., 1999). In this study and previous studies (Sidibé et al., 1997), we have demonstrated that this functional specificity is also maintained by pallidal and nigral projections that reach CM/Pf in monkeys. For instance, our findings clearly indicate that the CM innervates almost exclusively the sensorimotor striatum and receives specific inputs from the corresponding sensorimotor territory of GPi. On the other hand, the Pf projects preferentially to the nucleus accumbens/caudate nucleus and receives inputs from functionally corresponding regions of GPi and SNr (Sadikot et al., 1992; Sidibé et al., 1997). At the electron microscopic level, direct synaptic contacts were found between thalamostriatal neurons and GPi terminals, which confirms the existence of basal ganglia thalamostriatal loops. Therefore, these findings are consistent with the idea that part of the information flowing through the basal ganglia-thalamostriatal loops remains segregated in different channels (Fig. 9).

However, one must not consider these loops as carrying unprocessed information through closed circuits. There are various sites along the way where complex integrative processes may occur within and between loops. For instance, striatal interneurons definitely provide a route by which thalamostriatal information may be integrated and possibly transferred from one functional loop to another. The evidence that most striatal interneurons receive substantial inputs from CM/Pf combined with their extensive intrastriatal axonal arborization strongly supports this possibility (Kawaguchi et al., 1995; Sidibé and Smith, 1999). Another potential site for complex integration of thalamostriatal information is cross-talk between "direct" and "indirect" striatofugal neurons via intrinsic axon collaterals (Yung et al., 1996). Although CM inputs target preferentially direct striatofugal neurons (Sidibé and Smith, 1996), the fact that direct and indirect striatal cells are interconnected opens up the possibility of complex integrative processes taking place in the striatum.

Results from our recent study of GPi projections to CM/Pf have led to the subdivision of Pf into two parts, the Pf proper and the Pfdl (Sidibé et al., 1997). The Pfdl was defined as a dorsolateral extension of Pf that lies above the CM and receives almost exclusively pallidal projections from the dorsal one-third of GPi. Because this part of the nuclear complex was not seen as a separate entity in previous studies, very little is known about its synaptic inputs and projection sites. In the present study, we confirm that Pfdl receives a massive input from the caudate-receiving territory of GPi (dorsal one-third). However, most neurons in this region do not send reciprocal projections to the caudate nucleus but rather innervate the precommissural part of the putamen (Fig. 9). At present, it is difficult to speculate about the functional significance of these findings because of the lack of data relating to the specific connectivity and functions of the precommissural putamen and the Pfdl. In general, the precommissural putamen and caudate nucleus are considered as associative striatal territories because of their tight connections with associative cortices. Although there is slight variability in the source and pattern of distribution of cortical inputs to these two regions, both structures receive afferents from most associative areas in the frontal, temporal, and parietal lobes (Selemon and Goldman-Rakic, 1985; Cavada and Goldman-Rakic, 1991; Yeterian and Pandya, 1991, 1993, 1998). Consistently with this apparent homo-

geneity between the two regions, electrophysiological studies did not reveal any significant difference in responses to reward or generation of goal-directed movements among the anterior caudate nucleus, putamen, and ventral striatum (Romo et al., 1992; Schultz and Romo, 1992; Hassani et al., 2001). Thus, the functional implications of our anatomical observations await further studies of the anatomy and functions of the anterior striatum and Pfdl. Of course, we cannot rule out the possibility that some Pfdl neurons may also be connected with GPi neurons that receive inputs from the precommissural putamen. However, none of the putamen-receiving areas of GPi that have been injected with anterograde tracers in this and our previous study (Sidibé et al., 1997) led to substantial labeling in Pfdl, which suggests that the caudate-receiving territory of GPi is likely to be the most important source of pallidal inputs to this specific population of thalamostriatal neurons.

Functional roles of CM/Pf in basal ganglia circuitry

The exact roles played by thalamostriatal projections are still matters of speculation. However, anatomical data obtained over the past 10 years have clearly shown that these projections are massive and well organized and target specific populations of striatal neurons (Nakano et al., 1990; Francois et al., 1991; Sadikot et al., 1992; Groenewegen and Berendse, 1994; Sidibé and Smith, 1996; Sidibé et al., 1999). It is also important to note that the CM and Pf are not the sole sources of thalamostriatal projections. The rostral intralaminar nuclei and ventral motor thalamic nuclei also provide substantial inputs to the striatum (Groenewegen and Berendse, 1994; McFarland and Haber, 2000, 2001). However, it is unlikely that the information conveyed along the ventral thalamostriatal axons is the same as that flowing through the CM/Pf. The fact that many VA/VL neurons send axon collaterals to the striatum and cortex suggests that the ventral thalamostriatal pathway may serve as a positive feedback that integrates basal ganglia output and motor cortical information to dorsal striatal regions. On the other hand, inputs from CM/Pf may be important in supplying the striatum with attention-gated multimodal sensory information (Matsumoto et al., 2001). Recent data, indeed, have demonstrated that CM and Pf supply the tonically active neurons in the monkey striatum with information about behaviorally significant sensory events important for conditional responses (Matsumoto et al., 2001). For instance, CM/Pf inputs could provide information about appearance, disappearance, or change of attention-demanding behaviorally significant sensory events to striatal neurons (Matsumoto et al., 2001). Such a hypothesis is consistent with positron emission tomographic imaging studies in humans showing increased cerebral blood flow in CM when humans go from a relaxed, awake state to an attention-demanding reaction-time task (Kinomura et al., 1996). Various brainstem inputs from attention-related regions, such as the reticular formation, pedunculopontine tegmental nucleus, and superior colliculus, may contribute to these functional characteristics of CM/Pf neurons. However, one must be cautious in assuming that CM and Pf carry similar types of information to the striatum. As discussed above, these two nuclei receive strikingly different sets of cortical and subcortical inputs. Furthermore, Matsumoto et al. (2001) have recently shown that neurons in Pf respond faster than CM neurons to behaviorally significant sensory events in monkeys trained to learn and perform sensorimotor tasks. Although the functional significance of these observations remains to be established, they should be kept in mind when considering the role of the thalamostriatal projection from caudal intralaminar nuclei in primates.

ACKNOWLEDGMENTS

We thank Frank Kiernan for photography and Peggy Plant for clerical work.

REFERENCES

Alexander GE, DeLong MR, Strick PL. 1986. Parallel organization of functionally segregated circuits linking basal ganglia and cortex. Ann Rev Neurosci 9:357–381.

Balercia G, Kultas-Ilinsky K, Bentivoglio M, Ilinsky IA. 1996. Neuronal and synaptic organization of the centromedian nucleus of the monkey thalamus: a quantitative ultrastructural study, with tract tracing and immunohistochemical observations. J Neurocytol 25:267–288.

Beckstead RM, Domesick VB, Nauta WJH. 1979. Efferent connections of the substantia nigra and ventral tegmental area in the rat. Brain Res 175:191–217.

Carpenter MB, Nakano K, Kim R. 1976. Nigrothalamic projections in the monkey demonstrated by autoradiographic technics. J Comp Neurol 165:401–416.

Cavada C, Goldman-Rakic PS. 1991. Topographic segregation of corticostriatal projections from posterior parietal subdivisions in the macaque monkey. Neuroscience 42:683–696.

De las Heras S, Mengual E, Gimenez-Amaya JM. 1998. Overlapping territories between the thalamostriatal and nigrothalamic projections in cats. Neuroreport 9:1913–1916.

Deschênes M, Bourassa J, Van Diep D, Parent A. 1996a. A single-cell study of the axonal projections arising from the posterior intralaminar thalamic nuclei in the rat. Eur J Neurosci 8:329–343.

Deschênes M, Bourassa J, Parent A. 1996b. Striatal and cortical projections of single neurons from the central lateral thalamic nucleus in the rat. Neuroscience 72:679–687.

Fenelon G, Francois C, Percheron G, Yelnik J. 1991. Topographic distribution of the neurons of the central complex (centre-median-parafascicular complex) and of other thalamic neurons projecting to the striatum in macaques. Neuroscience 45:495–510.

Francois C, Percheron G, Yelnik J, Tande D. 1988. A topographic study of the course of nigral axons and of the distribution of pallidal axonal endings in the center median-parafascicular complex of macaques. Brain Res 473:181–186.

Gerfen CR, Staines WA, Arbuthnott GW, Fibiger HC. 1982. Connections of the substantia nigra in the rat. J Comp Neurol 207:283–303.

Gimenez-Amaya JM, McFarland NR, Heras S, Haber SN. 1995. Organization of thalamic projections to the ventral striatum in the primate. J Comp Neurol 354:127–149.

Groenewegen HJ, Berendse HW. 1994. The specificity of the nonspecific midline and intralaminar thalamic nuclei. Trends Neurosci 17:52–57.

Groenewegen HJ, Galis-de Graaf Y, Smeets JAJ. 1999. Integration and segregation of limbic cortico-striatal loops at the thalamic level: an experimental tracing study in rats. J Chem Neuroanat 16:167–185.

Hallanger AE, Levey AE, Lee HJ, Rye DB, Wainer BH. 1987. The origins of cholinergic and other subcortical afferents to the thalamus in the rat. J Comp Neurol 262:105–124.

Hassani OK, Cromwell HC, Schultz W. 2001. Influence of expectation of different rewards on behavior-related neuronal activity in the striatum. J Neurophysiol 85:2477–2489.

Ilinsky IA, Kultas-Ilinsky K. 1990. Fine structure of the magnocellular subdivision of the ventral anterior thalamic nucleus (VAmc) or *Macaca mulatta*. I. Cell types and synaptology. J Comp Neurol 294:455–478.

Ilinsky IA, Jouandet ML, Goldman-Rakic PS. 1985. Organization of nigrothalamocortical system in the rhesus monkey. J Comp Neurol 236:315–330.

Ilinsky IA, Tourtellotte WG, Kultas-Ilinsky K. 1993. Anatomical distinctions between two basal ganglia afferent territories in the primate motor thalamus. Stereotact Funct Neurosurg 60:62–69.

Joel D, Weiner I. 1994. The organization of basal ganglia-thalamocortical

circuits: open interconnected rather than closed segregated. Funct Neurosurg 60:70–79.

Jones EG. 1985. The thalamus. New York: Plenum Press.

Kawaguchi Y, Wilson CJ, Augood SJ, Emson PC. 1995. Striatal interneurons: chemical, physiological, and morphological characterization. Trends Neurosci 18:527–535.

Kinomura S, Larsson J, Gluyas B, Roland PE. 1996. Activation by attention of the human reticular formation and thalamic intralaminar nuclei. Science 271:512–515.

Kultas-Ilinsky K, Ilinsky IA. 1990. Fine structure of the magnocellular subdivision of the ventral anterior thalamic nucleus (Vamc) of *Macaca mulatta*: II. Organization of nigrothalamic afferents as revealed with EM autoradiography. J Comp Neurol 294:479–489.

Kultas-Ilinsky K, Ilinsky IA. 1991. Fine structure of the ventral lateral nucleus (VL) of the Macaca mulatta thalamus: cell types and synaptology. J Comp Neurol 314:319–349.

Liu XB, Jones EG. 1991. The fine structure of serotonin and tyrosine hydroxylase immunoreactive terminals in the ventral posterior thalamic nucleus of cat and monkey. Exp Brain Res 85:507–518.

Macchi G, Bentivoglio M, Molinari M, Minciacchi D. 1984. The thalamocaudate versus thalamo-cortical projections as studied in the cat with fluorescent retrograde double labeling. Exp Brain Res 54:225–239.

Matsumoto N, Minamimoto T, Graybiel AM, Kimura M. 2001. Neurons in the thalamic CM-Pf complex supply striatal neurons with information about behaviorally significant sensory events. J Neurophysiol 85:960–976.

McFarland NR, Haber SN. 2000. Convergent inputs from thalamic motor nuclei and frontal cortical areas to the dorsal striatum in the primate. J Neurosci 20:3798–3813.

McFarland NR, Haber SN. 2001. Organization of thalamostriatal terminals from the ventral motor nuclei in the macaque. J Comp Neurol 429:321–336.

Mengual E, de las Heras S, Erro E, Lanciego JL, Gimenez-Amaya JM. 1999. Thalamic interaction between the input and the output systems of the basal ganglia. J Chem Neuroanat 16:185–197.

Nakano K, Hasegawa Y, Tokushige A, Nakagawa TS, Mizuno N. 1990. Topographical projections from the thalamus, the subthalamic nucleus, and pedunculopontine tegmental nucleus to the striatum in the Japanese monkey *Macaca mulatta*. Brain Res 537:54–68.

Olucha F, Martinez-Garcia F, Lopez-Garcia C. 1985. A new stabilizing agent for tetramethylbenzidine (TMB) reaction product in the histochemical detection of horseradish peroxidase (HRP). J Neurosci Meth 13:131-138

Paré D, Smith Y, Parent A, Steriade M. 1988. Projections of brainstem core cholinergic and non-cholinergic neurons of cat to intralaminar and reticular thalamic nuclei. Neuroscience 25:69–86.

Parent A. 1990. Extrinsic connections of the basal ganglia. Trends Neurosci 13:254–258.

Parent A, DeBellefeuille L. 1983. The pallidointralaminar and pallidonigral projections in primate as studied by retrograde double-labeling method. Brain Res 278:11–27.

Percheron G, Filion M. 1991. Parallel processing in the basal ganglia: up to a point [letter, comment]. Trends Neurosci 14:55–59.

Powell TPS, Cowan WM. 1956. A study of thalamo-striate relations in the monkey. Brain 79:364–390.

Romo R, Scarnati E, Schultz W. 1992. Role of primate basal ganglia and frontal cortex in the internal generation of movements. II. Movement-related activity in the anterior striatum. Exp Brain Res 91:385–395.

Royce GJ. 1983. Single thalamic neurons which project to both the rostral cortex and caudate nucleus studied with the fluorescent double labeling method. Exp Neurol 79:773–784.

Royce GJ, Bromley S, Gracco C. 1991. Subcortical projections to the centromedian and parafascicular thalamic nuclei in the cat. J Comp Neurol 306:129–155.

Sadikot AF, Parent A, François C. 1992a. Efferent connections of the centromedian and parafascicular thalamic nuclei in the squirrel monkey: A PHA-L study of subcortical projections. J Comp Neurol 315:137–159.

Sadikot AF, Parent A, Smith Y, Bolam JP. 1992b. Efferent connections of the centromedian and parafascicular thalamic nuclei in the squirrel monkey: a light and electron microscopic study of the thalamostriatal projection in relation to striatal heterogeneity. J Comp Neurol 320: 228–242.

Sakai ST, Patton K. 1993. Distribution of cerebellothalamic and nigrothalamic projections in the dog: a double anterograde tracing study. J Comp Neurol 330:183–194.

Sakai ST, Smith A. 1992. The distribution of nigrothalamic projections in the dog. J Comp Neurol 318:83–92.

Sakai ST, Inase M, Tanji J. 1996. Comparison of cerebellothalamic and pallidothalamic projections in the monkey (*Macaca fuscata*): a double anterograde labeling study. J Comp Neurol 368:215–228.

Sakai ST, Stepniewska I, Qi HX, Kaas JH. 2000. Pallidal and cerebellar afferents to pre-supplementary motor area thalamocortical neurons in the owl monkey: a multiple labeling study. J Comp Neurol 417:164–180.

Schell GR, Strick PL. 1984. The origin of thalamic inputs to the arcuate premotor and supplementary motor areas. J Neurosci 4:539–560.

Schultz W, Romo R. 1992. Role of primate basal ganglia and frontal cortex in the internal generation of movements. I. Preparatory activity in the anterior striatum. Exp Brain Res 91:363–384.

Selemon LD, Goldman-Rakic PS. 1985. Longitudinal topography and interdigitation of cortico-striatal projection in the rhesus monkey. J Neurosci 5:776–794.

Sidibé M, Smith Y. 1996. Differential synaptic innervation of striatofugal neurones projecting to the internal or the external segments of the globus pallidus by thalamic afferents in the squirrel monkey. J Comp Neurol 365:445–465.

Sidibé M, Smith Y. 1999. Thalamic inputs to striatal interneurons in monkeys: synaptic organization and co-localization of calcium binding proteins. Neuroscience 89:1189–1208.

Sidibé M, Bevan MD, Bolam JP, Smith Y. 1997. Efferent connections of the internal globus pallidus in the squirrel monkey: I. Topography and synaptic organization of the pallidothalamic projection. J Comp Neurol 382:323–347.

Sidibé M, Pare JF, Raju D, Smith Y. 2001. Anatomical and functional relationships between intralaminar thalamic nuclei and basal ganglia in monkeys. In: Faull RLM, Nicholson L, editors. IBAGS VII. New York: Plenum Press. (in press).

Smith Y, Parent A. 1986. Differential connections of caudate nucleus and putamen in the squirrel monkey (*Saimiri sciureus*). Neuroscience 18: 347–371.

Smith Y, Sidibé M. 1999. Functional interconnections between the caudal intralaminar nuclei and the striatopallidal complex in monkeys. Soc Neurosci Abstr 25:884.19.

Smith Y, Bennett BD, Parent A, Sadikot AF. 1994. Synaptic relationships between dopaminergic afferents and cortical or thalamic input at the single cell level in the sensorimotor territory of the striatum in monkey. J Comp Neurol 344:1–19.

Smith Y, Sidibé M, Pare JF. 2000. Synaptic inputs from the substantia nigra and the pedunculopontine nucleus to thalamostriatal neurons. Soc Neurosci Abstr 26:361.15.

Tseng GF, Royce J. 1986. A golgi and ultrastructural analysis of the centromedian nucleus of the cat. J Comp Neurol 245:359–378.

Tsumori T, Yokota S, Lai H, Yasui Y. 2000. Monosynaptic and disynaptic projections from the substantia nigra pars reticulata to the parafascicular thalamic nucleus in the rat. Brain Res 858:429–435.

Yeterian EH, Pandya DN. 1991. Prefrontostriatal connections in relation to cortical architectonic organization in rhesus monkeys. J Comp Neurol 312:43–67.

Yeterian EH, Pandya DN. 1993. Striatal connections of the parietal association cortices in rhesus monkeys. J Comp Neurol 332:175–197.

Yeterian EH, Pandya DN. 1998. Corticostriatal connections of the superior temporal region in rhesus monkeys. J Comp Neurol 399:384–402.

Yung KKL, Smith AD, Levey AI, Bolam JP. 1996. Synaptic connections between spiny neurons of the direct and indirect pathways in the neostriatum of the rat: evidence from dopamine receptor and neuropeptide immunostaining. Eur J Neurosci 8:861–869.